J. Coat. Technol. Res., **9** (2) 163–170, 2012
DOI 10.1007/s11998-009-9226-9

Synthesis and characterization of nanosized titanium dioxide and silicon dioxide for corrosion resistance applications

A. M. Kamalan Kirubaharan, M. Selvaraj, K. Maruthan, D. Jeyakumar

Abstract We are reporting the preparation and characterization of nano-titanium dioxide and silica. The corrosion resistance performance of these nanopigments in silicone as well as silicone–polypyrrole Interpenetrating Polymer Network has been evaluated by impedance spectroscopy. The capacitance and resistance exerted by this nanocomposite coating were compared with the microcomposite coating and found that the nanocomposite coatings has the resistance in the order of 10^8 Ω cm^2 in 3% sodium chloride solution, which is more than the microcomposite coating. The comparison of heat resistance performance of these composite coatings indicates that nanocomposite coatings exhibit higher heat resistance property than the microcomposite coatings.

Keywords Interpenetrating Polymer Network, Nanocomposite, Sol–gel method, Silicone resin, Impedance spectroscopy, XRD, FTIR technique

Introduction

Titanium dioxide (TiO_2) is one among the important inorganic pigments used in the plastics and paint industry.[1] TiO_2 exists mainly in three naturally occurring crystallographic forms, namely anatase, brooklite, and rutile. Rutile is much closer to aromatic packing in its crystal pattern, and it is more stable than anatase phase. The denser atomic crystal pattern of rutile TiO_2 causes it to have higher specific gravity and refractive index than the anatase phase.

In recent years, nano-TiO_2 material has attracted researchers, owing to improved optical property,[2] photo catalytic action,[3] and other special characteristics to coating.[4–7] The nano-TiO_2 incorporated composite coatings considerably improve the mechanical properties and enhance the thermal stability.[8] Nano-silicon dioxide was one among the nanomaterials that has been studied as the polymer composite[9–12] for corrosion protection. Recent studies proved that the conducting polymers are useful to protect the ferrous and nonferrous metals from corrosive atmosphere. Polyaniline (PANI)[13–15] and polypyrrole (PPy)[16–18] with suitable dopants have been studied extensively for corrosion protection. Silicone-based coatings have increased their attraction in the field of protective coatings for high temperature application.[19,20] Further, silicone-based IPNs are excellent in thermal as well as corrosion resistance properties.[21–23] Studies on the anticorrosion behavior of the coatings employing nanopigments as one of the ingredients are gaining importance recently due to technological implications. An attempt has been made to prepare nano-TiO_2 and SiO_2 materials and characterize them. The dispersion of these nanomaterials was achieved by paste formation and silane treatment to have the composite coating. The nano-TiO_2 was also incorporated with Interpenetrating Polymer Network (IPN) and coated on steel substrate. The coated panels were evaluated by electrochemical impedance measurements and high temperature resistance tests, and the details are discussed in this paper.

Materials and methods

Titanium(IV) butoxide (AR), cyclohexanol (AR), hexadecyl trimethyl ammonium bromide (AR), and

A. M. Kamalan Kirubaharan
Polymer Science Department, Anna University, Chennai, India

M. Selvaraj (✉), K. Maruthan, D. Jeyakumar
Central Electrochemical Research Institute, Karaikudi, India
e-mail: selvaraj_58@yahoo.co.in

trifluoroacetic acid (AR) were obtained from M/s Kemphosal (P) Ltd., India. Triethylamine (L.R), absolute ethanol, and tetraethylorthosilicate (TEOS) were supplied by M/s Qualigens Fine Chemicals Pvt. Ltd., India. Deionized water was used in this study.

Preparation of nano-TiO_2

Titanium(IV) butoxide was used to prepare nano-TiO_2 particles under solvolytic condition. Titanium(IV) butoxide (10 g) was dissolved in cyclohexanol and then added to a premixed solution of distilled water, cyclohexanol, and hexadecyltrimethyl ammonium bromide at room temperature. The solution was allowed to stand for 12 h to give TiO_2 particles using triethylamine as precipitant. These particles were recovered by centrifugation. The particles were washed three times with acetone and dried in an air oven at 353 K for 2 h. One portion of the sample was calcined at 773 K and another part with 1073 K for 2 h in an electric furnace.

Preparation of trifluoroacetic acid-capped TiO_2

The trifluoroacetic acid-modified TiO_2 nanoparticles (TF-TiO_2) were synthesized with the methods similar to that of Xue et al.[24] Trifluoracetic acid (11.4 g, 0.1 mol) was dissolved in ethanol (60.0 mL) at room temperature. A solution of titanium(IV) butoxide (34.0 g, 0.1 mol) in ethanol (20.0 mL) was heated to 333 K under stirring. To this solution, trifluoroacetic acid (11.4 g, 0.1 mol) in 60 mL of ethanol was added dropwise and refluxed for 2 h. Deionized water (7.5 mL) was slowly added to the reaction mixture and was heated at 353 K for 6 h.

After the ethanol and butanol were removed under pressure distillation, the remaining powder was kept in a degassed desiccator for 1 day to give TF-capped TiO_2 nanoparticles.

Preparation of nano-SiO_2

The sample was prepared in the following molar ratio of TEOS:C_2H_5OH:H_2O:HNO_3 = 5:80:400:5, respectively, and stirred at 900 rpm at 348 K for 2 h. After the process, the contents were cooled at 281 K in ice bath followed by stirring for 2 h. Finally, the white turbid solution was obtained, which was kept aside for one day. The turbid solution was heated at 333 K until dry to evaporate the prepared solution. Finally, the product was washed with ethanol and ground by using mortar. The prepared silicon dioxide powder was calcined at 973 K for 4 h.

Characterization of nanoparticles

X-ray diffraction method

The X-ray diffraction (XRD) pattern for these pigments confirms the crystalline nature. XRD measurements were carried out by using X'Pert PROPAN analytical, Syn master 793, The Netherlands. The software used for analyzing the data was High Score plus X'Pert data collector. The crystallite size was calculated using Scherrer's formula

$$D = 0.9\lambda/\beta\cos\theta,$$

where D is crystallite size, β is full width at half maxima (in radians), and λ is wave length of the x-rays.

Transmission electron microscopy

Transmission electron microscopy (TEM) was used to ascertain the surface morphology and agglomeration of the particles to each other. The TEM photographs were obtained by using Tecnai G20, The Netherlands.

Preparation of micropigmented coatings

The coating formulations of micropigmented composite coatings were prepared by using silicone resin as well as silicone–PPy IPN. A solution of 0.259 mole of silicone resin and 0.427 mole of pyrrole were mixed in xylene solvent using benzyl peroxide as initiator. This reaction mixture was conducted in a reaction vessel with the addition of dibutyltin dilaurate as catalyst. After 6 h of this reaction, xylene was distilled off and the IPN formed was collected and characterized. The formation of IPN was confirmed through the surface morphological study by atomic force microscope (AFM) technique. The AFM morphology showed that the IPN had smooth glossy and heterogeneous microstructures.[25] The silicon resin used for this preparation was nondrying type with molecular weight 4000. The pigments used for this formulation were commercial TiO_2 and SiO_2 with the pigment loading of 15 PVC. The particle size of these materials was in the range of few microns. These formulations were prepared by using an attritor to get the Hegmann value of 8 and stored in an airtight container.

Preparation of nanopigmented coatings

The nanocomposite coatings were also prepared by using silicone resin and silicone–PPy IPN as binders. The pigments used for these nanocomposite coatings were nanosized titanium dioxide and silica with the pigment loading of 15 PVC as described in the previous section. These coating formulations were ground well

in an attritor to get the Hegmann's gage value of 8 and stored in a container.

Preparation of painted panels

Mild steel panels of size 7.5 cm × 5 cm were sandblasted to get Sa 2.5 of Swedish specification.[26] A set of sandblasted specimens were coated with the coating systems as shown in Table 1 along with the thicknesses of these coatings. After complete curing, these panels were evaluated for corrosion resistance as well as heat resistance tests.

Evaluation of coated specimen

Electrochemical impedance spectroscopy (EIS) measurements

Impedance measurements were carried out at open circuit potential using a Princeton Applied Research (PAR) Model 6310. A.C. impedance system consists of a three-electrode configuration. This system combines a lock-in amplifier for high frequency data measurements and a Fast Fourier Transformation computation scheme for low frequency analysis. The impedance measurements in all cases were carried out over a frequency range of 10 MHz to 100 KHz using a 10-mV peak-to-peak sinusoidal voltage. A computerized semicircle fitting routine was used to analyze the experimental data.

The electrochemical tests were carried out in a quiescent aerated 3% saline solution. The surface area of the coated panels exposed to the electrolyte was 1 cm^2. A three-electrode electrochemical cell was made by sticking a glass tube on the panels and filling it with the solution of the corrosive electrolyte (3% saline solution). A high surface area platinum mesh and saturated calomel electrode were used as counter and reference electrodes, respectively.

Heat resistance test

Heat resistance tests were carried out as per ASTM standard D2485. The panel was placed in a muffle furnace maintained at 478 K for 8 h. The temperature was increased in 55 K increments and maintained for 16 h. At the end of particular temperature, the panels were removed from the muffle furnace and the surface was examined for the formation of either cracks or charring and the observation was recorded.

Results and discussion

Characterization of nano-titanium dioxide and nano-silica

The nanoparticles were characterized by using XRD and TEM.

X-ray diffraction of TiO_2 and SiO_2 nanoparticles

The TiO_2 synthesized by the salvo thermal reaction was sintered at 773 and 1073 K. The powder XRD patterns of the samples are presented in Figs. 1 and 2, respectively. It can be seen from Fig. 1 that the diffraction lines are broad and well defined. The diffraction lines were compared with the standard and found to match with the anatase phase (ICDD No. 894921). Likewise, for the product sintered at 1073 K, the lines are sharp (Fig. 2) and the values are compared with standard pattern. In this case, most of the lines correspond to that of anatase, and trace quantity of rutile phase is also seen (ICDD No. 890555). There is a trace quantity of additional peak at 24.2 which could not be attributed to either anatase or rutile phase and may arise due to impurity. It can be seen from the figure that for the material annealed at 773 K, the FWHM values are higher than the material sintered at 1073 K. The crystallite sizes of these materials were calculated from the FWHM values and observed that the values correspond to 22 nm for the sample sintered at 773 K and 40 nm for the sample sintered at 1073 K.

Figure 3 shows the XRD pattern of SiO_2 particles calcined at 973 K. It is observed from the figure that the 2θ value exerted for the particles are 20.6° with d spacing of 4.3 A corresponding to the crystalline particles of silicon dioxide.

TEM analysis

TEM images of nano-TiO_2 particles and TF-capped TiO_2 particles are shown in Figs. 4 and 5, respectively. TEM image (Fig. 4) indicates that TiO_2 nanoparticles

Table 1: Coating system on sandblasted mild steel substrate

S. no.	Coating system	Coating formulation	Dry film thickness (μm)
1.	System 1	Silicone resin with rutile TiO_2 (micron)coating	40 ± 5
2.	System 2	Silicone resin with rutile TiO_2 (nano)coating	40 ± 5
3	System 3	Silicone–PPy IPN with rutile TiO_2 (micron)coating	40 ± 5
4	System 4	Silicone–PPy IPN with rutile TiO_2 (nano)coating	40 ± 5

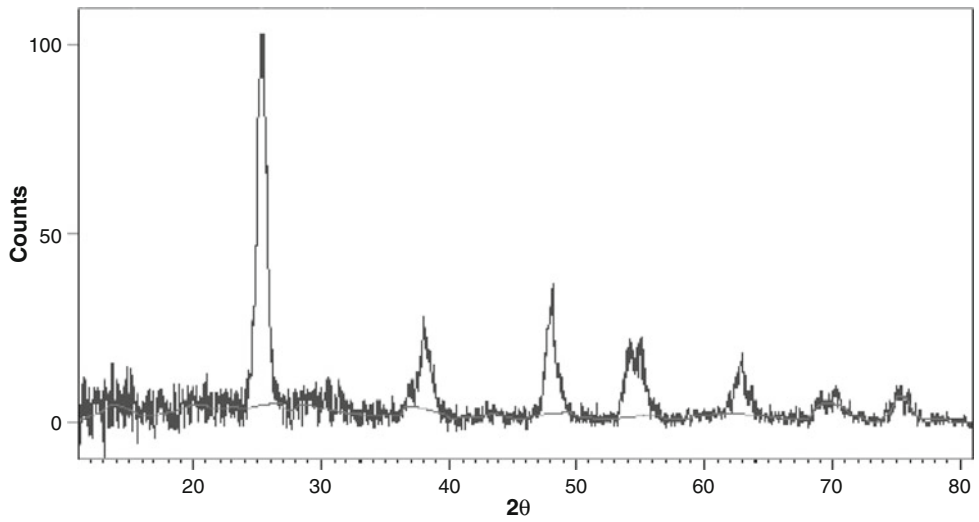

Fig. 1: XRD pattern of TiO_2 sintered at 773 K

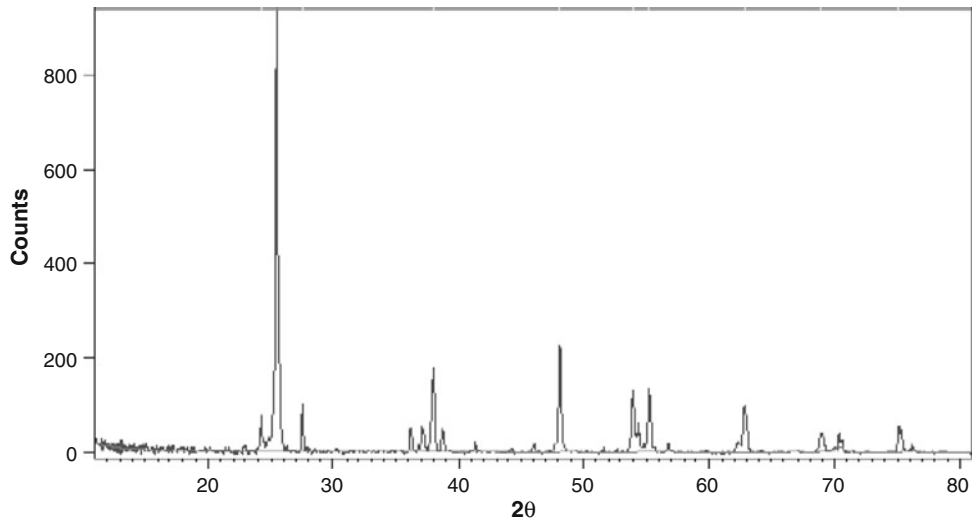

Fig. 2: XRD pattern of TiO_2 sintered at 1073 K

are extensively agglomerated and the grain boundaries are well defined though the individual particles could not be seen, indicating the crystalline nature of the material. Whereas, regarding the TF-capped TiO_2 (Fig. 5), the particle size was found to be around 20 nm, corroborating the crystallite size calculated from the XRD data. These particles have well-ordered tetragonal structure, which is in good agreement with the result of XRD. TEM reveals that the particles are highly crystalline. The cluster formation of TiO_2 particles are due to the tiny water molecules and hydroxyl group are unavoidable on nanoparticles. Thus, it is easy for nano-TiO_2 particles to heavily agglomerate in organic solvent or resin. (Surface-active agent can be adsorbed on nanoparticles by its hydrophilic ends. Organic acid and alcohols can react with the surface –OH groups on particles.) This may yield properties of the nanoparticle-filled composite that are even worse than those of microparticle/polymer system. To overcome these disadvantages, the agglomerated nanoparticles are loosened by being modified with trifluoroacetic acid and used for coating formulation.

Figure 6 shows the TEM micrograph of silica particles. The micrograph indicates that the formation of uniform size nanocrystalline SiO_2 is a thin layer surrounded by crystals of nano-SiO_2 particles. This is clearly shown in the figure by the black dense part followed by glassy gray colored crystalline SiO_2 particles. The Matsura et al.[27] study of high resolution TEM reveals that the iron oxide present in the composite coating is passivating the nano-silica particle and this facet is developing stronger on the sandblasted surface.

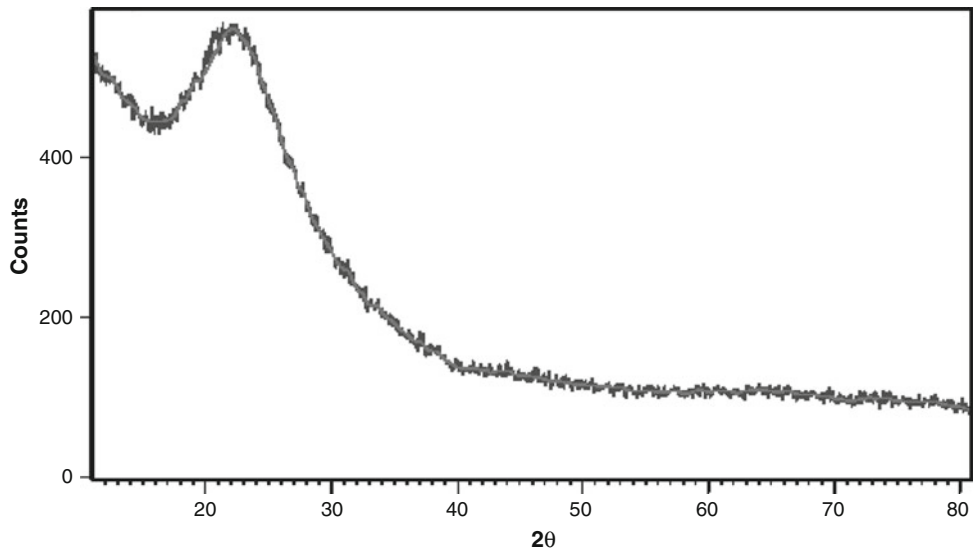

Fig. 3: XRD pattern of SiO_2 sintered at 923 K

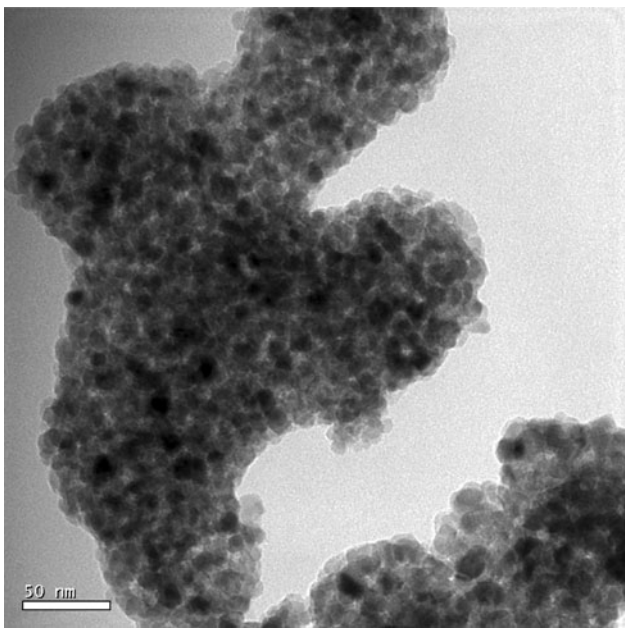

Fig. 4: TEM picture of nanocrystalline TiO_2

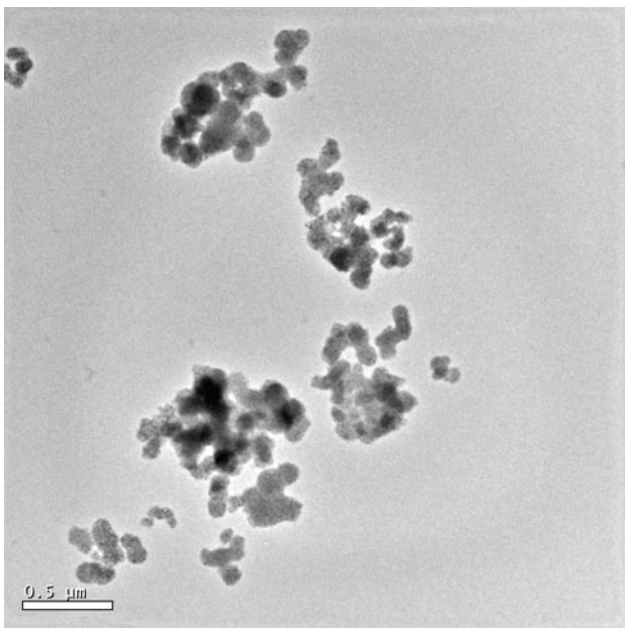

Fig. 5: TEM picture of TF-capped nanocrystalline TiO_2

Evaluation of coated specimen by EIS study

Figures 7 and 8 show the Bode plots of systems 2 and 4 on mild steel substrate and exposed in 3% sodium chloride solution for different durations. The capacitance and resistance exerted by the coated steels are given in Tables 2 and 3. It is seen from the figures that the reaction is diffusion controlled type with vertical slope at high frequency and horizontal slope in low frequency area. This indicates that at high frequency range the charge transfer reaction takes place between the electrolyte and the coating system. The low frequency is meant for the reaction between the interface of metal and the polymer layer. These plots are inclined toward the frequency axis with duration. In general, mild steel in 3% NaCl solution has a resistance between 120 and 180 Ω cm^2, dependent upon the composition of the metal. In this study, the resistance produced by the mild steel substrate in the NaCl solution is 130 Ω cm^2. All the coating systems on mild steel substrate produced very high resistance in the initial stage; however, it decreased with time and

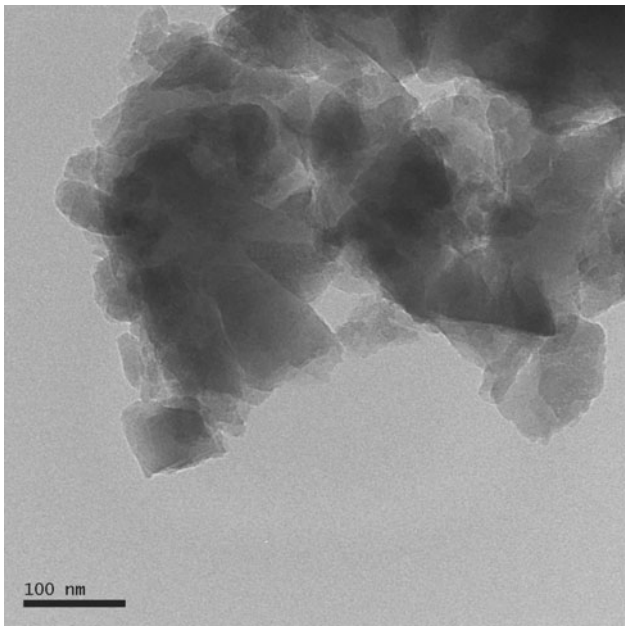

Fig. 6: TEM picture of nanocrystalline SiO_2

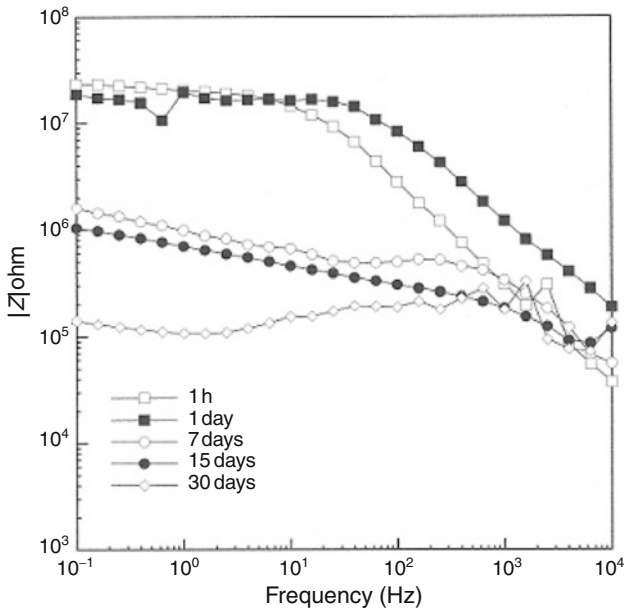

Fig. 7: Bode impedance plot of coating system 4 on mild steel substrate in 3% sodium chloride solution for different duration

reached 10^4 Ω cm^2 for micron size titanium dioxide pigmented systems (systems 1 and 3) at the tenure of 30 days. However, the nano-titanium dioxide incorporated systems 2 and 4 exerted high resistance 10^5 Ω cm^2 and 10^7 Ω cm^2, respectively, for the same duration.

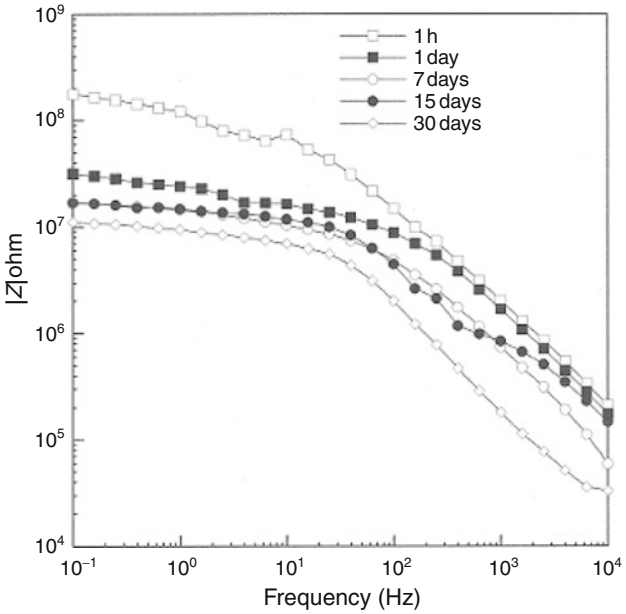

Fig. 8: Bode impedance plot of coating system 2 on mild steel substrate in 3% sodium chloride solution for different duration

By comparing the impedance data of silicone resin-based systems 1 and 2 (Table 2), it is observed that the R_t value of nano-TiO_2 pigmented coatings are higher than the system 1. The capacitance values from the impedance diagram that are associated with the water uptake by the coatings have been found to increase during initial stage of immersion. The capacitance (C_{dl}) values increase with time as the coating system slowly allows the penetration of ions and moisture.[28,29] Further, this is explained with the coatings limiting the corrosion process by a diffusion barrier-type mechanism. As seen in Table 2, it is evident that the nanocomposite silicone coating system has superior corrosion protection compared to the microcomposite system. This is due to the pore-free packing of the nano-titanium dioxide pigment in the composite coating systems.

The R_t and C_{dl} values of micron composite system 3 and nanocomposite silicone–PPy IPNs (system 4) are given in Table 3. From the table, it is shown that the R_t values of the nanopigmented coatings are higher than the micropigmented coatings. The C_{dl} value of system 3 increases with duration, whereas for system 4, it is an almost constant value throughout the period of the study. This suggests that the coating is limiting the corrosion process by a diffusion barrier-type mechanism. The resistance of this system 4 is in higher order. From this result, it is confirmed that the nano-titanium dioxide incorporated coating shows superior corrosion resistance properties than the micron-size titanium dioxide incorporated coating.

Table 2: Resistance and capacitance obtained from the Bodes plot of silicone-composite coatings on MS substrate in 3% NaCl solution

Duration	Coating system 1		Coating system 2	
	R_t (Ω)	C_{dl} (F/cm^2)	R_t (Ω)	C_{dl} (F/cm^2)
1 h	9.702×10^6	1.456×10^{-9}	2.771×10^7	3.004×10^{-10}
1 day	9.929×10^5	2.027×10^{-9}	2.351×10^7	4.452×10^{-10}
7 days	1.261×10^5	3.339×10^{-9}	1.885×10^6	2.797×10^{-10}
15 days	8.078×10^4	1.084×10^{-9}	9.784×10^5	6.827×10^{-9}
30 days	5.123×10^4	1.024×10^{-9}	0.925×10^5	7.776×10^{-9}

Table 3: Impedance data of silicone–PPy IPN micro- and nanocomposite coatings on MS substrate in 3% NaCl solution

Duration	Coating system 3		Coating system 4	
	R_t (Ω)	C_{dl} (F/cm^2)	R_t (Ω)	C_{cdl} (F/cm^2)
1 h	1.084×10^8	8.849×10^{-10}	2.223×10^8	4.557×10^{-11}
1 day	7.235×10^7	7.780×10^{-10}	3.967×10^7	7.791×10^{-11}
7 days	1.037×10^5	5.022×10^{-9}	2.466×10^7	1.206×10^{-10}
15 days	6.238×10^4	4.072×10^{-9}	2.427×10^7	1.027×10^{-10}
30 days	2.213×10^4	2.012×10^{-9}	1.107×10^7	1.002×10^{-10}

High temperature resistance properties

The coated specimens were subjected to heat treatment as per the ASTM specification D2485, and the failure of the coatings was observed visually by color change, chalking, cracking, and loss of adhesion. The micro- as well as nanosize pigmented silicone-based systems 1 and 2 withstood up to 698 K. Thereafter at 753 K, failure of the coating was observed. The stability of the coatings at the temperature 698 K was due to the formation of a cohesive bond between the binder and the pigment to form a hard adhesive mass over the steel surface. However, at 753 K, the cohesive bond between the surface and the coating broke down followed by oxidation of the steel substrate.

The heat-resistance performance of micro- as well as nanocomposite IPNs slightly differed from the silicone-based coating systems. The micropigmented coating system 3 withstood up to 753 K. The gloss of the coating system did not change at this temperature. The next temperature range at 808 K, the coating failed with the formation of cracks on the surface. However, the nanocomposite coating system withstood at 808 K. The gloss and color of the coating system did not changed at this temperature. But failures of this system were observed at 863 K. Thus, the cohesive bond formed between the coating and the substrate was hard and stable for this system at 808 K, which failed at 863 K and failed to protect the substrate. The heat resistance test indicates that the nanopigmented composite IPN coatings have superior heat-resistance properties compared with the micropigmented IPN system.

Conclusion

Nano-titanium dioxide and nano-silicon dioxide pigments have been prepared by sol–gel method and characterized by XRD and TEM micrographs. All the studies indicate that the particle size of anatase TiO_2, rutile TiO_2, and SiO_2 are 10, 40, and 92 nm, respectively.

Micro- as well as nanocomposite coating systems were formulated and evaluated for the corrosion as well as heat resistance properties. Nanocomposite coating based on silicone–PPy–IPN exhibited very high resistance in the order of 10^7 Ω cm^2 after 30 days of immersion in sodium chloride solution. This high resistance offered by the nanocoating system is substantial evidence for their very high corrosion resistance compared to the other systems. Similarly, nanosize pigment incorporated IPN coatings have superior heat-resistance performance compared with the micro-size pigment incorporated coating system.

References

1. Lim, BC, Thomas, NL, Sutherland, I, ''Surface Energy Measurements of Coated Titanium Dioxide Pigment.'' *Prog. Org. Coat.*, **62** 123–128 (2008)
2. Fukuji, S, Kazuaki, H, Kazuaki, Y, Yukio, M, Yoshitoma, T, ''Preparation and Optical Properties of Titanium Dioxide Iridescent Pigment Based on Black Titanium Oxynitride.'' *J. Jpn Soc. Colour Mater.*, **79** 526–532 (2006)
3. Fujishima, A, Zhong, X, Tryk, DA, ''TiO_2 Photocatalysing and Related Surface Phenomena.'' *Surf. Sci. Rep.*, **63** 515–582 (2008)

4. Li, HY, Chen, YF, Ruan, CX, Gao, WM, Xie, YS, ''Preparation of Organic–Inorganic Multifunctional Nanocomposite Coating via Sol–Gel Routes.'' *J. Nano Part. Res.*, **3** 157–160 (2001)
5. Xu, T, Xie, CS, ''Tetrapod-Like Nano-Particle ZnO/Acrylic Resin Composite and Its Multi-function Property.'' *Prog. Org. Coat.*, **46** 297–301 (2003)
6. Allen, NS, Edge, M, Ortega, A, Sandoval, G, Lianw, CM, Veeran, J, Stratton, J, McIntyre, RB, ''Degradation and Stabilization of Polymers and Coatings: Nano Versus Pigmentary Titania Particles.'' *Polym. Degrad. Stab.*, **3** 927–946 (2004)
7. Diamandesan, L, Vasillin, F, Tarabasanu-Mihaita, D, Fedar, M, Vlaicu, AM, Teodorescu, CM, Macuvei, D, Enculescu, I, Parvulescu, V, Vasile, E, ''Structural and Photocatalytic Properties of Iron and Europium-Doped TiO_2 Nano Particles Obtained Under Hydrothermal Conditions.'' *Mater. Chem. Phys.*, **112** 146–153 (2008)
8. Shi, H, Liu, F, Yang, L, Han, E, ''Characterization of Protective Performance of Epoxy Reinforced with Nanometer-Sized TiO_2 and SiO_2.'' *Prog. Org. Coat.*, **62** 359–368 (2008)
9. Pavlidou, S, Papaspyrides, CD, ''A Review on Polymer Layered Silicate Nano Composites.'' *Prog. Org. Coat.*, **33** 1119–1198 (2008)
10. Li, X, Wang, G, Li, X, ''Surface Modification of Nano SiO_2 Particles Using Polyaniline.'' *Surf. Coat. Technol.*, **197** 56–60 (2005)
11. Xiong, M, Wu, L, Zhou, S, You, B, ''Preparation and Characterization of Acrylic Latex/Nano-SiO_2 Composites.'' *Polym. Int.*, **51** 693–698 (2002)
12. Amerio, E, Fabbri, P, Malucelli, G, Messori, M, Sangermano, M, Taurino, R, ''Scratch Resistance of Nano-Silica Reinforced Acrylic Coatings.'' *Prog. Org. Coat.*, **62** 129–133 (2008)
13. Bernard, MC, Joiret, S, Hugot-Le Goft, A, Viet Phong, P, ''Protection of Iron Against Corrosion Using a Polyaniline Layer by Polyaniline Electrodeposition.'' *J. Electrochem. Soc.*, **148** (1) B12–B16 (2001)
14. Troch-Nagles, G, Winard, R, Wevmeersch, A, Renard, L, ''Electron Conducting Organic Coating on Mild Steel by Electropolymerization'' *J. Appl. Electrochem.*, **22** 756–764 (1992)
15. Syed Azim, S, Sathiyanarayanan, S, Venkatachari, G, ''Anticorrosive Properties of PANI-ATMP Polymer Containing Organic Coating.'' *Progr. Org. Coat.*, **56** (2–3) 154–158 (2006)
16. Ateh, DD, Navsaria, HA, Vadgama, P, ''Polypyrrole-Based Conducting Polymers and Interaction with Biological Tissues.'' *J. R. Soc. Interf.*, **3** 741–751 (2006)
17. Nguyen Thile, M, Bernard, MC, Garcia-Renaud, B, Deslouis, C, ''Raman Spectroscopy Analysis of Polypyrrole Films as Protective Coatings on Iron.'' *Synth. Met.*, **140** (2–3) 287–293 (2004)
18. Hosseini, MG, Sabouri, M, Shahrabi, T, ''Corrosion Protection of Mild Steel by Polypyrrole Phosphate Composite Coating.'' *Prog. Org. Coat.*, **60** 178–185 (2007)
19. Mukherjee, AK, Bhattia, SS, Pande, LM, ''Silicone Based Air Drying Heat and Corrosion Resistant (Sea Water) Aluminium Paint.'' *Paint India*, **25** 15–21 (1975)
20. Finzel, WA, ''High Solids Polyorganosiloxane Polymers for High Temperature Application.'' *J. Coat. Technol.*, **64** 47–50 (1992)
21. Dhoke, SK, Palraj, S, Maruthan, K, Selvaraj, M, ''Preparation and Characterization of Heat Resistant Interpenetrating Polymer Net Work (IPN).'' *Prog. Org. Coat.*, **59** 21–27 (2007)
22. Ananda Kumar, S, Sankara Narayanan, TSN, ''Thermal Properties of Siliconized Epoxy Interpenetrating Coating.'' *Prog. Org. Coat.*, **45** 323–330 (2002)
23. Rohwerder, M, Michalic, A, ''Conducting Polymers for Corrosion Protection: What makes the Difference Between Failure and Success?'' *Electrochem. Acta*, **53** 1300–1313 (2007)
24. Xue, Q, Liu, W, Zhang, Z, ''Friction and Wear Properties of a Surface Modified TiO_2 Nanoparticle as an Additive in Liquid Paraffin.'' *Wear*, **213** 29–32 (1997)
25. Kirubaharan, K, Selvaraj, M, Palraj, S, Rajagopal, G, ''Synthesis and Characterization of High Temperature Resistance IPN.'' *J. Appl. Polym. Sci.* (communicated)
26. Venison, JR, *Structural Steel Painting: The International Decorative Paints*, Allen Davies and Co. Ltd., Bristol, England (1973) p. 5
27. Matsura, V, Guari, Y, Larionova, J, Guérin, C, Caneschi, A, Sangregorio, C, Lancelle-Beltran, E, Mehdi, A, Corriu, RJP, ''Synthesis of Magnetic Silica-Based Nanocomposites Containing Fe_3O_4 Nanoparticles.'' *J. Mater. Chem.*, **14** 3026–3033 (2004)
28. Hladky, K, Callow, LM, Dawson, JL, ''Corrosion Rate from Impedance Measurement: An Introduction.'' *Brit. Corros.*, **15** 20–25 (1980)
29. Louis Floyd, F, Avudiappan, S, Gibson, J, Mehta, B, Smith, P, Provder, T, Escarsega, J, ''Using Electrochemical Impedance Spectroscopy to Predict the Corrosion Resistance of Unexposed Coated Metal Panels.'' *Prog. Org. Coat.*, **66** (1) 8–34 (2009)